still interacts with Arp2/3, we do not know whether Arp2/3 binds to a composite site including elements from both the VCA and B-GBD fragments (as modeled in Fig. 2D), or if it only interacts with the B-GBD site. We only know that the second binding site helps shift the VCA-Arp2/3 complex into a nonproductive conformation.

32. M. G. Rudolph *et al.*, *J. Biol. Chem.* **273**, 18067 (1998).
33. Simulation of cooperativity model. The fractional activity of N-WASP was calculated to be

$$\theta = \frac{K_B[A] + K_A[B] + c[A][B]}{K_A K_B + K_B[A] + K_A[B] + c[A][B]}$$

where [W] is the concentration of mini–N-WASP, [A] is the total concentration of input molecule A, [B] is the total concentration of input molecule B, c is the cooperativity factor linking binding of A and B, and

$$K_A = \frac{[W][A]}{[W{\cdot}A]} \quad K_B = \frac{[W][B]}{[W{\cdot}B]}$$

$$\frac{K_A}{c} = \frac{[W{\cdot}B][A]}{[W{\cdot}A{\cdot}B]} \quad \frac{K_B}{c} = \frac{[W{\cdot}A][B]}{[W{\cdot}A{\cdot}B]}$$

This model assumes that $[W_{tot}] \ll [A]$ and $[B]$, and that species WA, WB, and WAB have equal activity (W is inactive). Theoretical curves describing the behavior for different values of c were calculated using the program Mathematica (Wolfram Research, www.wolfram.com).
34. R. Rohatgi, H. H. Ho, M. W. Kirschner, *J. Cell Biol.* **150**, 1299 (2000).
35. We thank J. Zalevsky for reagents and helpful discussions and H. Bourne, V. Denic, D. Julius, B. Kelch, H. Madhani, J. Weissman, and members of the Lim lab for comments and discussion. Supported by grants to W.A.L. from NIH, the Burroughs Wellcome Young Investigator Program, the Searle Scholars Program, and the Packard Foundation. K.E.P. is a Cancer Research Institute Postdoctoral Fellow.

20 July 2000; accepted 18 September 2000

Direct Coupling Between Meiotic DNA Replication and Recombination Initiation

Valérie Borde,[1] Alastair S. H. Goldman,[2] Michael Lichten[1]*

During meiosis in *Saccharomyces cerevisiae*, DNA replication occurs 1.5 to 2 hours before recombination initiates by DNA double-strand break formation. We show that replication and recombination initiation are directly linked. Blocking meiotic replication prevented double-strand break formation in a replication-checkpoint–independent manner, and delaying replication of a chromosome segment specifically delayed break formation in that segment. Consequently, the time between replication and break formation was held constant in all regions. We suggest that double-strand break formation occurs as part of a process initiated by DNA replication, which thus determines when meiotic recombination initiates on a regional rather than a cell-wide basis.

During meiosis in most organisms, division of the diploid genome among haploid gametes is accompanied by frequent recombination between homologous parental chromosomes. Recombination occurs after meiotic DNA replication but before the first meiotic division. In the yeast *Saccharomyces cerevisiae*, blocking meiotic replication has been shown to prevent recombination (*1*–*4*), but the connection between these two fundamental processes remains unknown. A replication dependence of meiotic recombination would be expected if replication-inhibited cells could not form the double-strand breaks (DSBs) that initiate recombination. This could result either from a direct coupling between replication and DSBs or from checkpoint systems that sense incomplete replication and prevent DSB formation.

To test these suggestions, we examined DSBs in cells undergoing meiosis in the presence of 100 mM hydroxyurea (HU), a concentration that prevents DNA replication (*4*). In such conditions, meiotic progression is normally blocked before the first nuclear division (meiosis I) by the *MEC1*-dependent checkpoint system; progression is restored in *mec1-1* mutants (*4*). Wild-type cells sporulated in HU did not form DSBs, and meiotic progression was blocked (*5*). By contrast, about 40% of *mec1-1* mutant cells progressed through the meiosis I in the presence of HU, but DSBs still did not form (Fig. 1). Thus, the failure to form DSBs without replication is not due to a *MEC1*-dependent checkpoint block to meiotic progression, making it likely that replication is directly required for DSB formation. This conclusion is reinforced by the finding that *clb5 clb6* double mutants, which prevent meiotic replication without inducing the *MEC1* block (*4*), also fail to form DSBs (*6*).

To further examine the relation between replication and DSBs, we used two methods to delay replication in the left arm of chromosome *III* (chr*III-L*). One approach used an *ars305 ars306 ars307* triple mutation to inactivate all meiotic replication origins on chr*III-L* (*7*) (Fig. 2A). The *ars305 ars306 ars307* chr*III-L* is replicated passively by forks initiating at *ARS309* on the right arm (chr*III-R*) or further to the right, at least 126 kb from the left-hand telomere. On the basis of a fork progression rate of 2 kb/min (*8*), replication of the *ars305 ars306 ars307* chr*III-L* should take at least 40 min longer than when these origins are present and active. The other approach used a reciprocal translocation (*his4::TEL1-L*, Fig. 2A), replacing the first 70 kb of chromosome *III* with the first 4 kb of chromosome *I* (*TEL1-L*). This places *TEL1-L* next to the *HIS4-CEN3* region, which undergoes frequent DSBs (*9*) and contains the early-firing origin *ARS306* (*10*). Yeast telomeres are late replicating and impose this property on nearby sequences (*11*, *12*), so this translocation should delay replication in the *HIS4-CEN3* region.

We monitored meiotic replication on chromosome *III* by two-dimensional (2D) gel electrophoresis of replication intermediates (*13*). Replication occurred simultaneously at three locations on the normal chromosome *III* (Fig. 2D). By contrast, in *ars305 ars306 ars307* strains, replication on chr*III-L* was delayed by 60 min relative to chr*III-R* (Fig. 2, B and D), as expected if chr*III-L* was replicated passively by forks initiating on chr*III-R*. On *his4::TEL1-L*, replication in the *HIS4-CEN3* region was delayed by 30 min relative to chr*III-R* (Fig. 2D), and most *ARS306* origin activity was eliminated (*5*), as expected for a telomere position effect on replication.

Delaying replication did not markedly affect DSB frequencies on chr*III-L*, as measured from blots of pulsed-field gels (Fig. 2C). Maximum DSB levels on the *ars305 ars306 ars307* chr*III-L* were identical to those on the normal chromosome (20% ± 6% compared with 20% ± 5%), as were break levels at individual sites (*5*). DSBs between *HIS4* and *CEN3* on *his4::TEL1-L* were modestly reduced (6 ± 2% compared with 12 ± 2% on a normal chromosome), the reduction being stronger near *TEL1* than near *CEN3*. However, delaying replication locally had a distinct, reproducible effect on DSB timing (Fig. 2, C and D). DSBs formed simultaneously (1.5 to 2 hours after replication) in both arms of the normal chromosome *III*. By contrast, overall DSB formation in the late-replicating *ars305 ars306 ars307* chr*III-L* was delayed by 30 min compared with chr*III-R* (Fig. 2, C and D). Thus, the time interval between replication and DSB formation was maintained in both arms. Furthermore, the DSB delay in the originless chr*III-L* varied with distance from active right-arm

[1]Laboratory of Biochemistry, Division of Basic Science, National Cancer Institute, Bethesda, MD 20892–4255, USA. [2]Department of Molecular Biology and Biotechnology, University of Sheffield, Sheffield S10 2TN, UK.

*To whom correspondence should be addressed. E-mail: lichten@helix.nih.gov

origins (Fig. 3), being greater at a centromere-distal site (*YCL49c*, 1-hour delay) than at a centromere-proximal site (*YCL10c*, 30-min delay). In the *his4::TEL1–L* chromosome, DSBs formed 30 min later in the late-replicating *his4-CEN3* interval than in the earlier replicating chr*III-R*, again maintaining a 2-hour gap between replication and DSBs (Fig. 2D). By contrast, the time of DSB repair was independent of the time of break formation. Early- and late-forming DSBs disappeared at the same time (Figs. 2C and 3B), and X-shaped recombination intermediates formed at the same time in early- and late-replicating sequences in *ars305 ars306 ars307* mutants (Fig. 2B) and in all other diploids examined (*5*).

These data indicate that, irrespective of the time of replication, a constant period of time is maintained between replication and DSB formation in a region. DSB repair, by contrast, occurs at a specific time during meiosis, suggesting that repair is controlled on a cell-wide basis. Further evidence that DSB timing does not affect repair was provided by measuring recombination between *leu2* mutant alleles (*leu2-K* and *leu2-R*) located between *HIS4* and *CEN3* (see Fig. 2A). Leu^+ meiotic recombinants were recovered from *his4::TEL1–L*, *ars305 ars306 ars307*, and control strains in 0.42, 0.45, and 0.40% of spores, respectively.

DSB frequencies are often measured with the use of mutants (*rad50S*, *mre11S*, *sae2/com1*) in which the protein that creates DSBs, Spo11p, remains covalently attached to break 5′ ends (*14*, *15*). Failure to remove Spo11p results in the accumulation of unrepaired breaks, which are more easily detected and quantified. We observed, in *sae2*Δ or *rad50S* mutants, a marked effect of replication timing on DSB frequencies (Fig. 4). In *ars305 ars306 ars307 sae2*Δ strains, total DSBs on the late-replicating chr*III-L* were reduced fourfold relative to a *sae2*Δ strain with all origins intact (Fig. 4A). Breaks in the late-replicating *HIS4-CEN3* region of *his4::TEL1-L sae2*Δ strains were reduced almost 10-fold (Fig. 4A); repression at

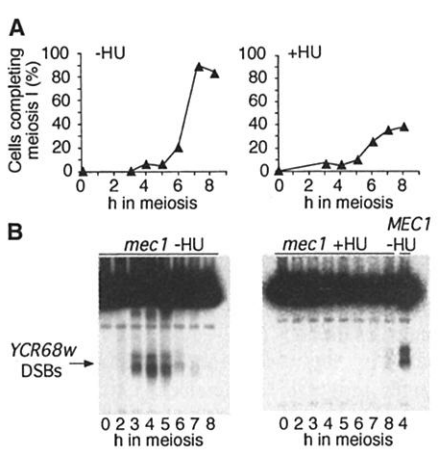

Fig. 1. DNA replication is required for DSB formation. A checkpoint-deficient *mec1-1/mec1-1* diploid was sporulated in the absence (−HU) or presence of 100 mM hydroxyurea (+HU), which blocks meiotic DNA replication (*4*, *26*). (**A**) Meiotic progression, monitored by fluorescence microscopy of 4′,6′-diamidino-2-phenylindole (DAPI)–stained cells. Cells with more than one nucleus were scored as having completed the first meiotic division. (**B**) DSB formation. Blots contain digested DNA extracted at the indicated time during meiosis (*26*). The rightmost lane contains meiotic DNA from an untreated wild-type control (MJL1071).

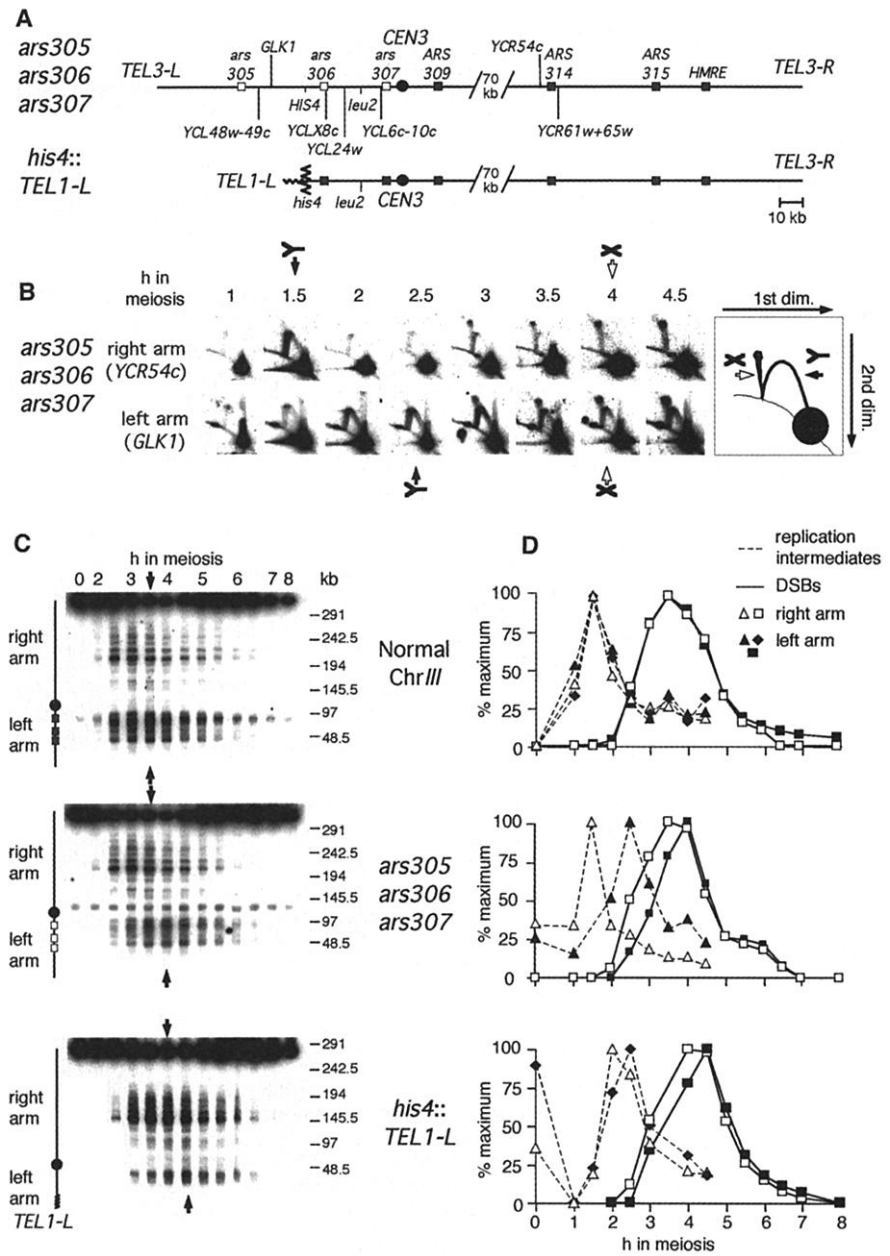

Fig. 2. DSB formation is delayed in late-replicating regions. (**A**) Map of chromosome *III*. Filled and open squares, functional and inactive origins, respectively, in *ars305 ars306 ars307* mutants; zig-zag line, breakpoint of the *his4::TEL1-L* translocation (*27*). (**B**) Meiotic replication intermediates in an *ars305 ars306 ars307* strain. 2D gel blots with DNA extracted at the indicated times were probed with left arm (*GLK1*) and right arm (*YCR54c*) probes (*27*). "Y" arc, replication intermediates; "X" spike, recombination intermediates (*28*); vertical arrows, time of maximum intermediate levels. (**C**) DSBs on whole chromosomes. Pulsed-field gel blots with DNA extracted at the indicated times were probed with left-end probes (*27*). Vertical arrows, time of maximum DSB levels in each arm. (**D**) Replication intermediate and DSB quantitation. Dotted lines, replication intermediates at *GLK1* (▲), at *ARS306* (◆), or at *YCR54c* (△). Solid lines, DSBs on the left arm (■) and on the right arm (□), measured on pulsed-field gels. The time that a strain initiates meiosis after transfer to sporulation medium varies between cultures. In the experiments presented here, measurements of the time of nuclear divisions indicate that the *his4::TEL1-L* strain initiated meiosis 1 half-hour later than did the other two strains (*5*).

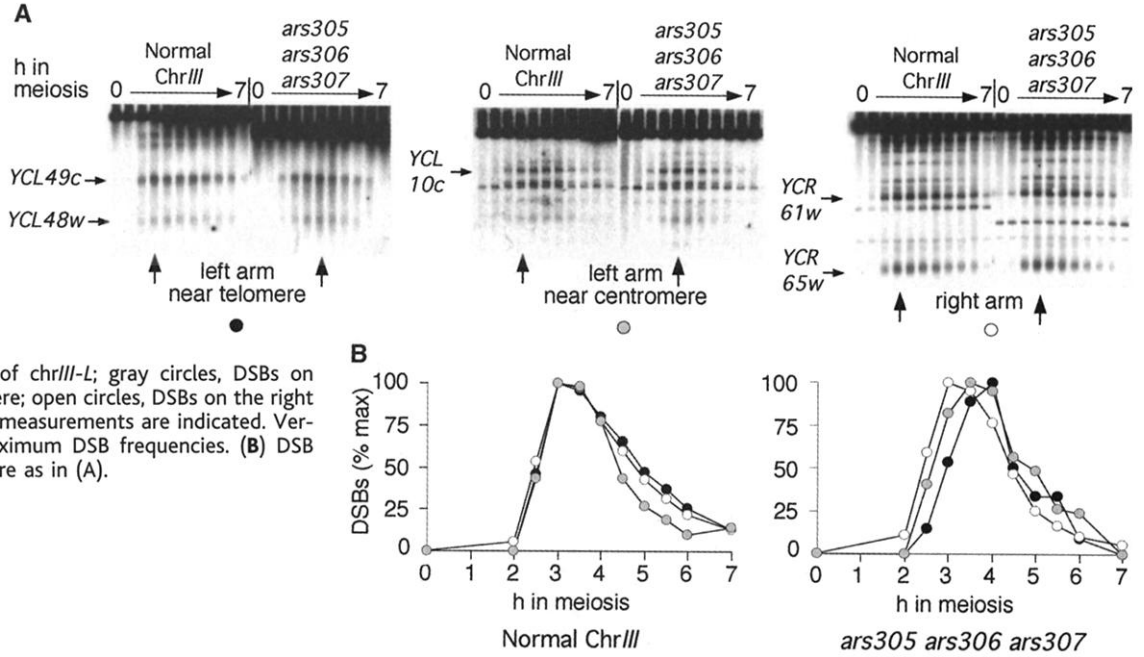

Fig. 3. The DSB delay increases with distance from active origins. DSBs were measured at individual sites with conventional agarose gels (*26*). (**A**) DSBs at individual sites. Blots containing restriction-digested DNA from wild-type and *ars305 ars306 ars307* cells at 0, 2, 2.5, 3, 3.5, 4, 4.5, 5, 5.5, 6, and 7 hours in meiosis. Solid circles, DSBs near the left end of chr*III-L*; gray circles, DSBs on chr*III-L* near the centromere; open circles, DSBs on the right arm. DSB bands used for measurements are indicated. Vertical arrows, time of maximum DSB frequencies. (**B**) DSB quantification. Symbols are as in (A).

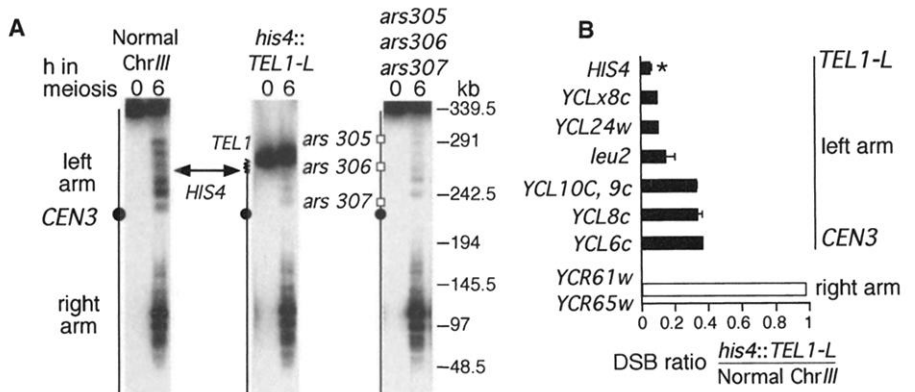

Fig. 4. Breaks are reduced in late-replicating regions in the absence of DSB processing. (**A**) DSBs on whole chromosomes in *sae2*Δ strains (*26*). Pulsed-field gel blots with DNA prepared at 0 or 6 hours in meiosis, hybridized with a chromosome *III* right-end probe. Total DSB frequencies in each chromosome arm are given. (**B**) *sae2*Δ-specific DSB reduction at individual sites. Frequencies at individual sites were measured with blots of conventional agarose gels (*27*). Black bars, DSBs in the *HIS4-CEN3* region; open bar, DSBs on the right arm. Loci are arranged in terms of increasing distance from the left-hand telomere. *, DSBs at *his4* in *his4::TEL1-L sae2*Δ strains were below the limit of detection (0.05% of chromosomes); this ratio was calculated assuming 0.05% as an upper value.

individual sites increased with proximity to the new telomere (Fig. 4B). DSBs near the right-hand telomere of chromosome *III* were also differentially reduced in *sae2*Δ mutants (*5*). We speculate that this *sae2*Δ/*rad50S*-dependent reduction in late DSBs could be due to checkpoint systems that sense unprocessed DSBs and prevent later break formation. Alternatively, it could result from a failure to recycle a DSB-forming complex, thought to remain at DSB sites in the absence of processing (*16*). In either case, break measurements obtained with *rad50S* or *sae2* mutants should be interpreted cautiously, because these mutants specifically reduce DSBs in late-replicating regions.

In summary, our data confirm that meiotic replication is required for DSB formation. DSB formation is most likely directly coupled to replication because a fixed time period is maintained between these two events. DSB processing-defective mutants allow a further distinction between break formation in early- and late-replicating regions. Collectively, these findings identify meiotic DNA replication as the primary event governing DSB formation. Evidence for a replication-DSB interplay is also provided by recent findings that meiotic S phase is shortened in *spo11* deletion mutants (*17*). We suggest that DNA replication of a region initiates a series of events that culminate, 1.5 to 2 hours later, in DSB formation. This is in contrast to what is seen in bacteria or in vegetatively growing yeast, where recombination-initiating lesions are formed by fork pausing and breakage during replication itself (*18*).

DNA replication has been suggested as playing an important role in several chromosome structural changes that occur during mitotic growth of *S. cerevisiae*, including the establishment of sister chromatid cohesion (*19*), the restoration of transcriptional silencing to mating-type gene cassettes (*20*), and the recruitment of chromatin-remodeling factors (*21*). Our studies identify meiotic recombination as another chromosomal transformation coupled to DNA replication and thus provide evidence for a mechanistic link between these two fundamental processes. In meiosis, the 1.5- to 2-hour period observed between replication and DSB formation might reflect the time needed to assemble protein complexes that participate in DSB formation (*17*, *22*) or to establish interhomolog contacts needed for efficient DSB formation (*17*, *23*, *24*). Our findings indicate that such processes are coupled to replication on a regional basis, rather than by a cell-wide progression signal. The ability to create and distinguish between early- and late-replicating regions should allow the determination if other landmark events of meiosis, such as the assembly of early homolog pairing structures or the formation of synaptonemal complex, are also directly coupled to meiotic DNA replication and thus are affected by its timing.

References and Notes

1. G. Simchen, D. Idar, Y. Kassir, *Mol. Gen. Genet.* **144**, 21 (1976).
2. M. E. Budd, K. D. Wittrup, J. E. Bailey, J. L. Campbell, *Mol. Cell. Biol.* **9**, 365 (1989).
3. D. Schild, B. Byers, *Chromosoma* **70**, 109 (1978).
4. D. Stuart, C. Wittenberg, *Genes Dev.* **12**, 2698 (1998).
5. V. Borde, A. S. H. Goldman, M. Lichten, data not shown.
6. K. N. Smith, A. Penkner, K. Ohta, F. Klein, A. Nicolas, personal communication.
7. I. Collins, C. S. Newlon, *Mol. Cell. Biol.* **14**, 3524 (1994).
8. L. H. Johnston, D. H. Williamson, A. L. Johnson, D. J. Fennell, *Exp. Cell Res.* **141**, 53 (1982).
9. F. Baudat, A. Nicolas, *Proc. Natl. Acad. Sci. U.S.A.* **94**, 5213 (1997).
10. A. E. Reynolds, R. M. McCarroll, C. S. Newlon, W. L. Fangman, *Mol. Cell. Biol.* **9**, 4488 (1989).
11. R. M. McCarroll, W. L. Fangman, *Cell* **54**, 505 (1988).
12. B. M. Ferguson, W. L. Fangman, *Cell* **68**, 333 (1992).
13. B. J. Brewer, W. L. Fangman, *Cell* **51**, 463 (1987).
14. S. Keeney, C. N. Giroux, N. Kleckner, *Cell* **88**, 375 (1997).
15. H. Tsubouchi, H. Ogawa, *Mol. Cell. Biol.* **18**, 260 (1998).
16. T. Usui *et al.*, *Cell* **95**, 705 (1998).
17. R. S. Cha, B. M. Weiner, S. Keeney, J. Dekker, N. Kleckner, *Genes Dev.* **14**, 493 (2000).
18. R. Rothstein, B. Michel, S. Gangloff, *Genes Dev.* **14**, 1 (2000).
19. F. Uhlmann, K. Nasmyth, *Curr. Biol.* **8**, 1095 (1998).
20. A. M. Miller, K. A. Nasmyth, *Nature* **312**, 247 (1984).
21. K. Shibahara, B. Stillman, *Cell* **96**, 575 (1999).
22. K. Ohta *et al.*, *Proc. Natl. Acad. Sci. U.S.A.* **95**, 646 (1998).
23. V. Rocco, A. Nicolas, *Genes Cells* **1**, 645 (1996).
24. L. Xu, N. Kleckner, *EMBO J.* **14**, 5115 (1995).
25. Supplemental data are available at www.sciencemag.org/feature/data/1052791.shl.
26. All strains are diploids of the SK1 background, homozygous for the indicated mutations. Complete genotypes, construction details, and protocols for sporulation and conventional agarose gel analyses are available on *Science* Online (*25*).
27. The *ars305 ars306 ars307* diploid contains mutations inactivating *ARS305*, *ARS306*, and *ARS307*. The *his4::TEL1* diploid contains a reciprocal translocation with breakpoints at *HIS4* on chromosome *III* and at *PHO11* on chromosome *I*. Genotypes, construction details, and protocols for pulsed-field and 2D gel analyses are available on *Science* Online (*25*).
28. I. Collins, C. S. Newlon, *Cell* **76**, 65 (1994).

29. We thank C. Newlon and D. K. Bishop for strains; T. Allers for valuable advice; K. Smith, A. Nicolas, and C. Newlon for personal communications; and D. Chattoraj, J. Haber, G. Hayhurst, C. Newton, R. Shroff, B. Thomas, and M. Yarmolinsky for comments that improved this manuscript.

2 June 2000; accepted 10 August 2000

Genomic Analysis of Gene Expression in *C. elegans*

A. A. Hill,[1]* C. P. Hunter,[2]* B. T. Tsung,[2] G. Tucker-Kellogg,[1]† E. L. Brown[1]

Until now, genome-wide transcriptional profiling has been limited to single-cell organisms. The nematode *Caenorhabditis elegans* is a well-characterized metazoan in which the expression of all genes can be monitored by oligonucleotide arrays. We used such arrays to quantitate the expression of *C. elegans* genes throughout the development of this organism. The results provide an estimate of the number of expressed genes in the nematode, reveal relations between gene function and gene expression that can guide analysis of uncharacterized worm genes, and demonstrate a shift in expression from evolutionarily conserved genes to worm-specific genes over the course of development.

The nematode *C. elegans* is a genetically accessible model organism that is widely used to study genetics, development, and other biological processes (*1, 2*). In 1998, the genome of this organism was completely sequenced, and the presence of 19,099 genes, or open reading frames (ORFs), was predicted. This made it possible to use oligonucleotide arrays for genome-wide gene expression monitoring in this metazoan (*3, 4*). We designed three oligonucleotide arrays (denoted A, B, and C) to monitor the mRNA expression levels of 18,791 (98%) of the predicted worm ORFs; the remaining ORFs were not included because they were almost identical to one or more of the selected ORFs (*5*). To maximize the number of detected transcripts, we quantitated nematode gene expression in six developmentally staged populations from eggs to adult worms, in isolated oocytes, and in aged worms near the end of their ~2-week lifespan (*6*). We anticipated that the resulting data set would provide insight into gene expression in the nematode and also serve as a baseline for further experiments in *C. elegans*.

The number of ORFs called "present" by the Affymetrix GeneChip software (*7*) in any readout across all RNA samples is summarized in Table 1. In total, 10,747 ORFs (56%) were detected in at least one hybridization. This number of detected genes is comparable to the ~10,000 independent genes represented by the current set of *C. elegans* expressed sequence tags (ESTs) (*8*). We detected most ORFs with ESTs, and most of the ORFs that we did not detect are likely transcripts in very low abundance. For example, we detected 78% of the ORFs on the A array, which had sequence homology to *C. elegans* cDNAs. In contrast, 90% of the ORFs that we failed to detect are represented by at most a single cDNA in the *C. elegans* database ACEDB (version WS6).

Our ability to detect genes as expressed is dependent on many factors, but the most important two are the sensitivity of the oligonucleotide chip and the relative abundance of the transcripts. To estimate the sensitivity of the oligonucleotide arrays, we included in vitro synthesized transcripts in each hybridization (Table 1) (*9*). As determined by the signal response from these control transcripts, the sensitivity of detection of the arrays ranged between ~1:300,000 and 1:50,000. By way of example, we estimate that embryos contain ~10^7 transcripts (*10*); thus, a sensitivity level of 1:300,000 corresponds to detecting a gene expressed at an average of 30 transcripts per embryo. To be reliably detected, transiently expressed genes would need to be expressed at higher levels. Furthermore, as the animal grows, rare transcripts, particularly those expressed in only a few or single cells, would be further diluted by ubiquitous and abundant transcripts. Indeed, preliminary data from isolated gonads indicates the presence of many gonad- and germ line–specific messages that were at low or undetectable levels in whole worms (*11*). Thus, many of the ~8400 ORFs that were not detected in any experiment are probably genes that are expressed at levels below our limits of detection. Consistent with this, in a separate series of experiments that monitored expression in worms grown under stressful conditions (which should induce gene expression), we detected 611 additional transcripts that were not detected during the unperturbed life cycle (*11*).

By applying a one-way analysis of variance (ANOVA) to our replicated measurements, we isolated the subset of transcripts that had a significant ($P < 1 \times 10^{-3}$) increase or decrease in frequency (*12*) at some point during the life cycle and that were called "present" at least once; 4221 (22%) of the ORFs met these criteria. The expression profile of each of these developmentally modulated genes was normalized to have a mean value of zero and a variance of one, and the normalized profiles were clustered by means of a self-organizing map (SOM) (*13*). Examples of selected clusters are shown in

[1]Department of Genomics, Genetics Institute, Cambridge, MA 02140, USA. [2]Department of Molecular and Cellular Biology, Harvard University, Cambridge, MA 02138, USA.

*To whom correspondence should be addressed. E-mail: ahill@genetics.com (A.A.H.) and hunter@mcb.harvard.edu (C.P.H.)

†Present address: Millennium Predictive Medicine, 700 One Kendall Square, Third Floor, Cambridge, MA 02139, USA.